Published in final edited form as:
Dev Cell. 2012 April 17; 22(4): 763–774. doi:10.1016/j.devcel.2012.01.019.

Short-Term Integration of Cdc25 Dynamics Controls Mitotic Entry during *Drosophila* Gastrulation

Stefano Di Talia[1] and **Eric F. Wieschaus**[1,*]

[1]Howard Hughes Medical Institute, Department of Molecular Biology, Princeton University, Princeton, NJ 08544, USA

SUMMARY

Cells commit to mitosis by abruptly activating the mitotic cyclin-Cdk complexes. During *Drosophila* gastrulation, mitosis is associated with the transcriptional activation of *cdc25*^{string}, a phosphatase that activates Cdk1. Here, we demonstrate that the switch-like entry into mitosis observed in the *Drosophila* embryo during the 14th mitotic cycle is timed by the dynamics of Cdc25^{string} accumulation. The switch operates as a short-term integrator, a property that can improve the reliable control of timing of mitosis. The switch is independent of the positive feedback between Cdk1 and Cdc25^{string} and of the double negative feedback between Cdk1 and Wee1. We propose that the properties of the mitotic switch are established by the out-of-equilibrium properties of the covalent modification cycle controlling Cdk1 activity. Such covalent modification cycles, triggered by transcriptional expression of the activating enzymes, might be a widespread strategy to obtain reliable and switch-like control of cell decisions.

INTRODUCTION

During the cell cycle, a series of biochemical switches govern a cell's progression through major regulatory checkpoints (Morgan, 2007). At the onset of mitosis, the final G2/M checkpoint induces a reorganization of the cytoskeleton, nuclear membrane and chromatin structure to prepare for sister chromatids segregation. All these processes depend on a single group of master regulators: the mitotic cyclin-Cdk complexes.

In most cell types, entry into mitosis is triggered by an abrupt switch-like activation of cyclin-Cdk1 complexes (Morgan, 2007; O'Farrell, 2001). Cdk1 complexes are initially held in an inactive state by inhibitory phosphorylation of the Cdk1 subunit (mediated by the kinases Wee1 and Myt1). At the onset of mitosis, the abrupt removal of this phosphorylation (mediated by the phosphatase Cdc25) leads to the activation of Cdk1 (Morgan, 2007; O'Farrell, 2001). In human cells activation of Cdk1 triggers different mitotic events at different levels of kinase activity (Gavet and Pines, 2010). Although these mechanisms are well conserved among eukaryotes, the strategies that cells use to trigger Cdk1 activation and entry into mitosis differ in various organisms (Morgan, 2007).

During *Drosophila* gastrulation, entry into mitosis is associated with and requires transcriptional activation of *cdc25*^{string} (Edgar and O'Farrell, 1989, 1990). *cdc25*^{string} expression is sufficient to induce dephosphorylation of Cdk1 and to trigger mitosis (Edgar

*Correspondence: efw@princeton.edu.

SUPPLEMENTAL INFORMATION Supplemental Information includes Supplemental Experimental Procedures, five figures, and six movies and can be found with this article online at doi:10.1016/j.devcel.2012.01.019.

and O'Farrell, 1990). Mitosis 14 in the *Drosophila* embryo is executed in a reproducible and accurate spatiotemporal pattern consisting of 25 spatially distinct domains (Foe, 1989), providing a dramatic example of the precision with which the cell cycle can be programmed during development (Edgar and O'Farrell, 1990; O'Farrell, 2001). However, how expression of *cdc25*^{string} results in abrupt activation of Cdk1 and precise timing of cell division in *Drosophila* remains unknown. It has been proposed from experiments in *Xenopus* egg extract and mammalian cells that the abrupt activation of Cdk1 at the onset of mitosis is controlled by two feedback loops: a positive feedback loop between Cdc25 and Cdk1 and a double negative feedback loop between Wee1 and Cdk1. Cdc25 activity is stimulated by Cdk1-dependent phosphorylation (Hoffmann et al., 1993; Izumi and Maller, 1993; Kumagai and Dunphy, 1992; Trunnell et al., 2011), whereas Wee1 activity is inhibited by Cdk1-dependent phosphorylation (McGowan and Russell, 1995; Mueller et al., 1995). Positive feedback between Cdc25^{string} and Cdk1 and double negative feedback between Wee1 and Cdk1 can produce the switch-like control of mitosis observed in the *Xenopus* egg extract (Izumi and Maller, 1993; Kim and Ferrell, 2007; Novak and Tyson, 1993; Pomerening et al., 2003, 2005; Sha et al., 2003; Solomon et al., 1990; Trunnell et al., 2011). These feedbacks might facilitate the unidirectionality of the transition by creating a hysteretic bistable system (Pomerening et al., 2003; Sha et al., 2003). Recent experiments in somatic cell extracts (Deibler and Kirschner, 2010) indicate that Wee1 activity might be stimulated by phosphorylation by low Cdk1 levels (Deibler and Kirschner, 2010; Harvey et al., 2005) and inhibited by high levels (Deibler and Kirschner, 2010), suggesting a more complicated control mechanism.

In fission yeast, it is possible to engineer a functional cell cycle oscillator lacking Cdc25 and Wee1 dependent controls, as well as other controls (Coudreuse and Nurse, 2010). However, the timing of such cell cycles is very noisy (Coudreuse and Nurse, 2010), reminiscent of the extremely variable quantized cell cycles observed in cells mutant for both *cdc25* and *wee1* (Sveiczer et al., 1996). These results suggest that, similarly to fission yeast, inputs from Cdc25 and Wee1 might be required to obtain the reliable timing of cell division observed during embryonic development. The role of positive feedback and other molecular mechanisms in ensuring such temporal precision remains unclear.

To characterize the molecular switch controlling entry into mitosis during *Drosophila* embryonic development we focused on the control of the 14th mitotic division that happens after the embryo has cellularized and gastrulation has begun. The pattern of mitosis is associated with the expression of *cdc25*^{string} that is established by the developmental program regulating overall patterning of the embryo (Edgar et al., 1994a; Edgar and O'Farrell, 1989, 1990).

We find that cell divisions inside individual mitotic domains are controlled in a precise and reproducible wave-like pattern. This wave-like pattern reflects the transcriptional activation of *cdc25*^{string} and is unlikely to depend on other cellular or developmental inputs. The rate of accumulation of Cdc25^{string} determines the time of cell division in a switch-like manner. The switch operates as a short-term integrator, so that the decision of mitosis is effectively controlled by the concentration of Cdc25^{string} integrated over a timescale of 2 min. Cdc25^{string} activates Cdk1 in an ultrasensitive manner and this ultrasensitivity does not require the positive feedback between Cdc25^{string} and Cdk1 or the double negative feedback between Wee1 and Cdk1. Mathematical modeling and theoretical analysis suggest that ultrasensitive activation of Cdk1 is controlled by a covalent modification cycle operating in the first-order regime and far from steady state. The predicted signaling properties of such a covalent modification cycle reproduce well the measured signaling properties of the mitotic switch.

RESULTS

cdc25^{string} Transcriptional Activation Controls the Timing of Cell Division in Individual Cells

Within a mitotic domain, cell divisions are not absolutely synchronous. This asynchrony may reflect inherent variability and noise, but could also in part arise from the fact that within each domain, mitosis starts in a single cell or in a small number of interior cells then spreads wave-like, in all directions, until it stops at the domain boundary (Foe, 1989). To characterize the properties of the wave-like divisions inside mitotic domains, we imaged embryos expressing His2Av-GFP with 20-s frame rate to determine the time of mitosis inside domains 1 and 5 (Figure 1A). We developed algorithms to track the coordinates of each cell at the onset of gastrulation and the time at which it divided (Figures 1C and 1D). On average, cells in mitotic domain 1 divide ~5 min before those in mitotic domain 5 (Figure 1B), but each domain shows a reproducible wave-like pattern (Figures 1E and 1F). In both domains 1 and 5, the pattern begins in the center of the domain and extends radially. Most of the variability in division within each domain is attributable to this wave-live pattern. Although it takes ~10 min for all the cells in either domain to divide, on a cell-to-cell basis, the deviation from the expected (smoothed) wave-like pattern in either domain is only 2 min (Figures 1G and 1H).

The wave may represent a secondary control of mitotic timing, independent of Cdc25^{string}, or it might be produced if *cdc25*^{string} expression were initiated within each domain in a wave-like pattern corresponding to the final progression of mitosis. To distinguish between these possibilities, we examined the dynamics of *cdc25*^{string} expression in living embryos using a transcriptional reporter expressing nuclear localized GFP (GFP-NLS, Figure 2A and Movie S1 available online) under the control of a *cdc25*^{string} enhancer that drives expression in mitotic domains 1 and 5 (Lehman et al., 1999) (Figure S1). We developed algorithms to track individual nuclei and to quantify in each the nuclear fluorescence intensity (Figure 2B) from the early phase of gastrulation to the entry into mitosis (see Figure 2C for the definition of timing of cellular events). Using a numerical fitting procedure (Skotheim et al., 2008), we could estimate the time of activation of *cdc25*^{string} transcription for most cells belonging to domain 1 and 5. This analysis shows that for each cell the timing of its division correlates with the timing of its activation of *cdc25*^{string} (Figure 2D). The time from *cdc25*^{string} activation to entry into mitosis is similar in all the cells inside the two domains regardless of when *cdc25*^{string} expression is activated (Figure 2E). These results imply that the wave-like pattern of mitosis observed inside domain 1 and 5 reflect the pattern of activation of *cdc25*^{string} rather than any additional control process that intervenes between *cdc25*^{string} expression and division. Therefore, we conclude that it is very unlikely that other cellular and developmental inputs play an important role in setting the timing of mitosis in these cells.

Cdc25^{string} Dynamics Controls the Timing of Entry into Mitosis

The wave-like pattern of initial *cdc25*^{string} expression does not explain the remaining variability in division pattern and does not provide insight into how Cdc25^{string} ultimately controls entry into mitosis. To investigate the relationship between mitotic entry and Cdc25^{string} levels, we used a Gal4/UAS expression system to drive Cdc25^{string}GFP uniformly in the embryo. Under our experimental conditions, Cdc25^{string}GFP begins to accumulate uniformly in all cells ~50 min after the 13th anaphase (Figures 3A and 3B and Movie S3) preceding the time when endogenous Cdc25^{string} is first detectable by about 20 min (Figures 2C and 3B). Cdc25^{string}GFP accumulates proportionally in the cytoplasm and inside nuclei (Figures 3C and 3D), indicating that measurements of nuclear concentrations are proportional to cytoplasmic and cellular concentrations.

Uniform Cdc25^{string}GFP expression overrides the more complicated spatiotemporal pattern of endogenous Cdc25^{string} and all ectodermal cells in the embryo enter mitosis at about the same time (Movie S2). Similar results have been reported by Edgar and O'Farrell (1990). Because Gal4 levels vary between embryos, there is some variability in the rate of Cdc25^{string} accumulation and, consequently, in when cell division occurs (Figure S2J). Approximately half of the embryos express Cdc25^{string} at level similar to WT, so that the interval from the beginning of Cdc25^{string}GFP accumulation to mitosis is similar to the interval between GFP accumulation and mitosis observed for the previously described reporter strains for mitotic domains 1 and 5 (Figure 3B). We restrict our analysis to these cases.

Using algorithms to track nuclei, measure fluorescence in individual cells (Figure 3E, n = 198) and to reconstruct the total concentration of Cdc25^{string}GFP from the fluorescence measurements (see Experimental Procedures, Supplemental Experimental Procedures, and Figure S2) we find that in a given embryo cells in different positions along the anterior-posterior axis accumulate Cdc25^{string}GFP at the same rate and respond very similarly to expression of Cdc25^{string}GFP (Figure 3F and Experimental Procedures). To determine if variability in the timing of mitotic entry correlates with the rate of accumulation of Cdc25^{string}GFP, we plot the duration of the period from the beginning of Cdc25^{string} accumulation to mitotic entry (defined as ΔT) as a function of the Cdc25^{string}GFP accumulation rate. We find that ΔT varies subtly in individual cells and correlates inversely with the rate of Cdc25^{string}GFP accumulation in that cell (Figures 3G and 3H). We also analyzed the timing of cell division in wild-type (WT) embryos and embryos heterozygous for *cdc25^{string}* (see Experimental Procedures). We detected a delay of ~5 min in the timing of cell division in embryos heterozygous for *cdc25^{string}* compared to WT embryos (Figure 3I), supporting the observation that Cdc25^{string} accumulation rate determines the timing of cell division. These results argue that the dynamics of Cdc25^{string} accumulation may account for the remaining variability in the control of entry in mitosis.

We then use this variability to investigate how Cdc25^{string} controls mitotic entry. We consider two simple models: mitotic entry might be triggered instantaneously in a given cell once Cdc25^{string} levels reach a specific threshold, or Cdc25^{string} activity might be integrated over time to regulate mitosis (Figure 4A). An instantaneous model predicts that the value of Cdc25^{string} at entry into mitosis is the same for all the cells independently of ΔT, whereas the integral is an increasing function of ΔT (that should scale linearly with ΔT). An integrated model predicts that the integral of Cdc25^{string} should be a constant, whereas the value of Cdc25^{string} at entry into mitosis should scale approximately as ΔT^{-1}. We measured the correlation between the concentration of Cdc25^{string} at the time of mitotic entry and the interval ΔT (Figures 4B and S3). We also measured the correlation between the integral of Cdc25^{string} concentration from the beginning of accumulation and the interval ΔT (Figures 4C and S3). Neither the instantaneous model, nor integrating levels from the beginning of expression can account for the control of entry into mitosis (Figures 4B and 4C and S3). The decision of entering mitosis can be fitted by an instantaneous model assuming that for each cell there is a 2 min delay between the decision of entering mitosis and chromosome condensation (Figures 4D and S3). An equivalently good fit is obtained if cells integrate the concentration of Cdc25^{string}GFP over timescales of ~2 min to make their decision of entering mitosis (Figure 4E; integration time = 2.1 ± 0.9min, see Figure S3). We favor the short-term integration model for reasons that we will elucidate below.

The Decision of Entering Mitosis Depends on Cdc25^{string} in an Ultrasensitive Manner

To gain further insights into the molecular mechanisms by which Cdc25^{string} regulates the cell cycle, we analyzed how the rate of cell division is determined by the "short-term" integrated concentration of Cdc25^{string}: I_{K*stg}. Similar results are obtained using Cdc25^{string}

concentration (or the concentration 2 min before chromosome condensation, Figure S4). In all cases, we find that Cdc25^{string} controls entry into mitosis in an ultrasensitive manner (Figure 5A).

We used two standard procedures to obtain quantitative parameters describing the ultrasensitive control of mitosis by Cdc25^{string}. In the first procedure, we fit the rate of cell division with a logistic function and then estimate the values of Cdc25^{string} concentration at which the rate of cell division is 0.1 ($S_{0.1}$) and 0.9 ($S_{0.9}$). We then use these two numbers (Koshland et al., 1966) to determine an apparent Hill coefficient:

$$n_H = \frac{\log(81)}{\log\left(\frac{S_{0.9}}{S_{0.1}}\right)}$$

Apparent Hill coefficients close to 1 are indicative of a hyperbolic response, whereas coefficients much larger than 1 indicate ultrasensitivity. We also use an alternative definition of sensitivity (Fell, 1992). Given a system for which one measures how a quantity y depends on a signal S, one can define the response coefficient, r, as:

$$r = \frac{d\log(y)}{d\log(S)} = \frac{Sdy}{ydS}$$

For a linear system: r = 1, whereas ultrasensitive systems are characterized by r > 1.

We find that the rate of division moves from 0.1 to 0.9 over a change in I_{K^*stg} of only 1.95, giving an apparent Hill coefficient: $n_H = 7 \pm 1$ (Figure 5A) and by an average response coefficient (<r > = 3.9) much larger than 1 (r range: 1.5–5.3, Figures 5B and 5C).

Part of the ultrasensitivity reflects the direct effect of Cdc25^{string} on the phosphorylated state of Cdk1. We characterized how Cdc25^{string} activates Cdk1, performing western blots of 59 individual embryos expressing uniform UAS-Cdc25^{string}GFP to measure the amount of inactive Cdk1, i.e., Cdk1-pY15, as a function of Cdc25^{string}GFP levels (Figure 5D). The amount of Cdk1-pY15 decreases sharply as the concentration of Cdc25^{string}GFP increases (Figure 5E), indicating that Cdc25^{string} activates Cdk1 in an ultrasensitive manner. Activation of Cdk1 by Cdc25^{string} can be well described by a Hill function with a coefficient $n_H = 3.1 \pm 0.9$ (Figure 5E). We attribute the remaining switch-like behavior of the division to a nonlinear dependency on Cdk1 activity (apparent Hill coefficient = 3.4 ± 0.9) (Figure 5F).

Ultrasensitive Control of Mitosis Does Not Require Positive Feedback

The phosphorylated state of Cdk1 depends on the balance between the phosphatase activity of Cdc25 and the kinase activity of Wee1, responsible for the inhibitory phosphorylation of Cdk1. Both Cdc25 and Wee1 are thought to be subject to feedback (see Introduction). To test the role of these feedbacks in the ultrasensitivity of the response, we constructed transgenic flies expressing mutant Cdc25^{string} and Wee1 (Cdc25^{string}-9AGFP and Wee1-9ACFP both under the control of the Gal4/UAS system) in which the Cdk1 consensus sites were mutated (S/TP mutated to AP). Mutation of Cdk1 consensus sites have been shown to affect the feedback between Cdk1 and Cdc25^{string} in *Xenopus* and mammalian cells (Izumi and Maller, 1993; Strausfeld et al., 1994) and the feedback between Cdk1 and Wee1 in *Xenopus* and budding yeast (Harvey et al., 2011; Kim et al., 2005; Okamoto and Sagata, 2007).

To analyze if the phosphorylatable and nonphosphorylatable forms of both proteins are functional and if mutation of the Cdk1 consensus sites altered the activity of Cdc25^{string} and Wee1 as expected, we analyzed the effect of zygotic expression of these proteins. Zygotic overexpression of both Wee1-CFP and Wee1-9ACFP cause delays in the timing of mitotic domains (Figures 6A and 6B), indicating that both proteins are functional. Wee1-9ACFP overexpression causes a longer delay than overexpression of Wee1-CFP (Figure 6B), as expected because mutation of the Cdk1 consensus sites should prevent Cdk1-dependent inactivation of Wee1 (Kim et al., 2005; Okamoto and Sagata, 2007). When expressed zygotically Cdc25^{string}-9AGFP induced uniform mitoses in a manner similar to Cdc25^{string} (Movies S3 and S4), indicating that this mutant form is functional. The mutant probably impairs the ability of Cdk1 to phosphorylate and activate Cdc25^{string}, as Cdc25^{string}-9AGFP is less effective than Cdc25^{string}GFP at driving mitosis in the presence of high levels of Wee19A-CFP (Figures 6C and 6D; to avoid complication from expression of endogenous Cdc25^{string}, we analyzed the mitotic timing in amnioserosa cells, which never express *cdc25^{string}* and thus normally never divide after the completion of cellularization).

To test the effect of the mutants on ultrasensitivity under physiological conditions, we selected embryo expressing Cdc25^{string}GFP and Cdc25^{string}-9AGFP at similar rate (and at a rate similar to WT; see Figures 3D and 6E) and compared the dependency of the rate of cell division on the concentration of either form of Cdc25^{string}GFP. Control of mitotic entry has a similar ultrasensitive dependency on Cdc25^{string}GFP and Cdc25^{string}-9AGFP (apparent Hill coefficients ≈7 ± 1, average response coefficients ≈4 ± 1 for both curves; Figures 6G and 6J, S4 and S5, and Movie S4, N_{stgGFP} = 198 and $N_{stg9AGFP}$ = 233), indicating that the positive feedback between Cdc25^{string} and Cdk1 is not required for switch-like entry into mitosis. A slightly higher concentration of Cdc25^{string}-9AGFP (12%) is required for entry into mitosis.

To test the properties of the mitotic switch in the absence of both feedbacks, we analyzed the control of mitosis in embryos expressing Wee1CFP and Cdc25^{string}GFP or Wee1-9ACFP and Cdc25^{string}-9AGFP at levels similar to WT (Figure 6F; these embryos also express endogenous Wee1). We selected embryos that express Wee1CFP (or Wee1-9ACFP) only maternally and also express Cdc25^{string}GFP (or Cdc25^{string}-9AGFP) zygotically. In these conditions, Wee1CFP (or Wee1-9ACFP) concentration is almost constant during cycle 14, whereas Cdc25^{string}GFP (or Cdc25^{string}-9AGFP) accumulates as observed previously (Figure 6F). The rate of cell division shows a similar ultrasensitive dependency on Cdc25^{string} and Cdc25^{string}9A in embryos that express Cdc25^{string} and Wee1 or Cdc25^{string}9A and Wee19A (apparent Hill coefficients ≈7 ± 1, average response coefficients ≈4 ± 1 for both curves; Figures 6G–6J, S4 and S5, and Movies S5 and S6, $N_{stgGFPWee1CFP}$ = 148 and $N_{stg9AGFPWee19ACFP}$ = 110). The concentration of Cdc25^{string}-9AGFP required for entry into mitosis in embryos expressing both mutant proteins is slightly higher (17%) than the concentration of Cdc25^{string}GFP in embryos expressing both WT proteins (Figures 6G and S4). We interpret this shift (compatible with the existence of feedback; see also Figures 6A–6D) as a minor change in the properties of cell cycle control. These results, therefore, argue that switch-like activation of mitosis in response to Cdc25^{string} expression does not require any feedback mechanism between Cdk1 and Cdc25 and/or Wee1.

An Out-of-Equilibrium Covalent Modification Cycle Can Explain Feedback-Independent Ultrasensitivity

In the absence of feedbacks, the control of Cdk1 activity by Cdc25^{string} and Wee1 resembles a simple covalent modification cycle in which Cdk1 exists in unmodified and modified forms with the interconversion catalyzed by two converter enzymes (Cdc25^{string} and Wee1). An important question is how such a covalent modification cycle can produce switch-like changes in Cdk1 activity in the absence of feedbacks.

Although covalent modification cycles are widespread in signaling modules (Kholodenko, 2006), their properties have largely been analyzed at steady state where, in the absence of feedback loops, the cycle gives a hyperbolic activation of the substrate if the enzymes operate in the first-order regime but a switch-like activation if the enzymes are saturated (zero-order ultrasensitivity) (Goldbeter and Koshland, 1981). To investigate which regime might be relevant during activation of Cdk1, we measured the concentrations of Cdk1, $Cdc25^{string}$, and Wee1, because in zero-order kinetics substrate concentration should be in excess relative to that of enzymes and to the K_m of enzyme/substrate reaction (Goldbeter and Koshland, 1981). Using western blots of embryos and recombinant proteins we estimated the concentration of Cdk1 to be 240 ± 24 nM (Figure 7A), Cdk1 is saturated with cyclins in G2 of cycle 14 as indicated by its complete modification and the fact that Wee1-dependent phosphorylation requires cyclin association (Edgar et al., 1994b; Parker et al., 1991; Solomon et al., 1990). We, therefore, assume that the measured Cdk1 concentration approximates well the concentration of cyclin-bound Cdk1.

The concentrations of Wee1 (50 ± 10 nM) and $Cdc25^{string}$ (45 ± 10 nM, measured under conditions when half of Cdk1 is active) are only 5-fold lower than that of their substrate Cdk1 (Figures 7A–7C). Whether this is enough for zero-order ultrasensitivity depends on the enzymatic properties (K_m) of $Cdc25^{string}$ and Wee1. Estimates for human Cdc25s suggest that the measured concentration of Cdk1 is much lower than the K_m for the Cdc25/Cdk1 reaction ($K_m > 1\ \mu M$; see Experimental Procedures). These results imply that the dynamics of Cdk1 activation by $Cdc25^{string}$ should be well described by first-order kinetics. We lack precise measurements of the enzymatic properties of Wee1. However, as the concentration of Cdk1 is relatively low it is likely that Wee1 phosphorylation of Cdk1 also operates in the first-order regime. We, therefore, suggest that both enzymes operate in the first-order regime and that switch-like activation of Cdk1 cannot be attributed to zero-order kinetics.

One special feature of cell cycle control in *Drosophila* gastrula is that mitotic entry is driven by rapid accumulation of $Cdc25^{string}$ and may not be near equilibrium. To take this into account, we built a mathematical model of Cdk1 activation consisting of a covalent modification cycle in which $Cdc25^{string}$ is accumulating over time (Figure 7D). The unknown parameters of the model, relevant in the first-order regime, are the k_{cat}/K_m of Wee1 and $Cdc25^{string}$. Using the data of Cdk1 activation (Figure 5D) and numerical simulations, we estimated these parameters (Wee1: $k_{cat}/K_m = 10^5\ M^{-1}s^{-1}$, $Cdc25^{string}$: $k_{cat}/K_m = 2 \times 10^5\ M^{-1}s^{-1}$). Simulations of the model using these parameters indicate that the rapid accumulation of $Cdc25^{string}$ can produce switch-like activation of Cdk1 even when operating in the first-order regime (Figure 7E). Linear response theory indicates that this is at least in part due to the fact that the response time decreases as $Cdc25^{string}$ concentration increases (see below, Figure 7E, and Supplemental Experimental Procedures). To compare the model to the experimental data of Cdk1 activation (Figure 5E), we simulated it using the measured variable rates (and times) of $Cdc25^{string}$ accumulation (Figure 3). The model reproduces reasonably the curve of Cdk1 activation and the signaling properties of the mitotic switch (Figure 7F).

A Short-Term Integrator Controls Entry into Mitosis

The level of activated Cdk1 changes whenever the concentration of $Cdc25^{string}$ and Wee1 vary, but these changes are not instantaneous. The time required for Cdk1 to respond to changes in the concentration of $Cdc25^{string}$ and Wee1 reflects a property of the dynamical system controlling Cdk1 activity, termed response time (τ, Figure 7E). At every instant, the level of Cdk1 reflects in part its levels prior to the change and, therefore, the response time can be thought of as a time interval for temporal averaging. Tau can also be related to the typical time intervals that individual molecules of Cdk1 spend in a given phosphorylation

state (see Supplemental Experimental Procedures). From the standpoint of cellular decision-making, the response time is essentially analogous to an integration time, as shown by numerical simulations (Figures 7E and 7F).

Because the response time is determined by the time required for $Cdc25^{string}$ and Wee1 to act on Cdk1, it should depend on the concentrations of $Cdc25^{string}$ and Wee1. In the first-order regime the response time of a covalent modification cycle is well approximated by the expression: $\tau = (k_{wee1}[Wee1] + k_{Cdc25}[Cdc25])^{-1}$, where k_{Wee1} and k_{Cdc25} are the k_{cat}/K_m of Wee1 and Cdc25 (Detwiler et al., 2000; Gomez-Uribe et al., 2007). The model, therefore, predicts that it should be possible to change the response time (and as a consequence the integration time) by altering the levels of Wee1 (and as a result the levels of $Cdc25^{string}$ required for mitosis). Using embryos heterozygous for *wee1*, we analyzed the dependency of the integration time on Wee1 levels. The integration time is significantly increased in such embryos (Figures 7G and 7H, integration time = 5.8 ± 1.2 min) compatibly with the predictions of the model. Such an increase argues against a delay between the decision of entering mitosis and detectable chromosome condensation (which should only depend on pathways downstream of Wee1 and $Cdc25^{string}$). We also observe that the integration time is similar in embryos with or without feedback and slightly reduced by increase in Wee1 concentration as expected (Figure 8). This suggests that feedback does not play a role in setting the integration time and is unlikely to explain the change in integration time observed in *wee1* heterozygous embryos. Based on the above results, we propose that a short-term integrator controls the decision of entering mitosis and that the integration time is set by the time required for Cdk1 to respond to changes in $Cdc25^{string}$.

DISCUSSION

Control of Mitotic Entry by $Cdc25^{string}$

During *Drosophila* gastrulation, transcriptional activation of $cdc25^{string}$ is associated with entry into mitosis (Edgar and O'Farrell, 1989, 1990). Here, we have investigated how $Cdc25^{string}$ accumulation results in abrupt switch-like activation of Cdk1 and entry into mitosis. The time interval between $cdc25^{string}$ transcriptional activation and entry into mitosis is controlled by the rate of $Cdc25^{string}$ expression. The concentration of $Cdc25^{string}$ integrated over 2 min is the quantity that best correlates with the decision of entering mitosis and such integration time might be determined by the response time of Cdk1 activity to changes in $Cdc25^{string}$ concentration.

Two ultrasensitive steps (activation of Cdk1 by $Cdc25^{string}$ and entry into mitosis by Cdk1) control mitosis. Such a cascade can provide high ultrasensitivity from two moderately ultrasensitive steps. Positive feedback does not play an important role in the control of entry into mitosis in the *Drosophila* gastrula and we propose that the ultrasensitivity is rather due to the out-of-equilibrium properties of the covalent modification cycle controlling Cdk1. We observe that feedback mechanisms are conserved in *Drosophila* as it can be shown that mutants ($Cdc25^{string}$9A and Wee19A) that disable feedbacks have the expected effects on cell cycle control when overexpressed. This raises the question of why feedbacks do not play a role in WT cells. We propose that activation of mitosis in *Drosophila* is too rapid for feedback to make a significant contribution to Cdk1 activation. In *Xenopus* egg extract, positive feedback introduces a 10 min delay between the accumulation of cyclin to a critical threshold concentration and the activation of Cdk1 (Solomon et al., 1990). This delay has been interpreted as the time required to activate the feedback mechanism (Deibler and Kirschner, 2010; Solomon et al., 1990). Controlling entry into mitosis through rapid accumulation of $Cdc25^{string}$ is, therefore, likely to make the contribution of feedback irrelevant. When $Cdc25^{string}$9A ($Cdc25^{string}$) and Wee19A (Wee1) are overexpressed, the time between $Cdc25^{string}$ activation and mitosis can become significantly longer providing

enough time for feedback to contribute to activation of Cdk1. We speculate that the molecular network controlling entry into mitosis is highly flexible (O'Farrell, 2001) and can operate as cyclin-driven switch dependent on feedback or as Cdc25-driven switch with the properties described in this article. These two different strategies to control the cell cycle might reflect different selective pressures on the control of mitosis and might be utilized at different stages during development.

Precise Control of the Timing of Cell Divisions during Embryonic Development

The control of cell division during *Drosophila* gastrulation provides an extraordinary example of the temporal precision with which cell behaviors can be timed during embryonic development (Foe, 1989). This precision might be required to avoid incompatible cell behaviors that might easily arise due to the fast timescales of *Drosophila* embryonic development (Johnston, 2000). We suggest that controlling entry into mitosis by transcriptional expression of $cdc25^{string}$ rather than accumulation of cyclins avoids the possible delay due to activation of the positive feedback (Solomon et al., 1990). Such a delay might be incompatible with the precise control of cell divisions observed during *Drosophila* gastrulation. Positive feedback also has the potential of amplifying noise in the expression of $cdc25^{string}$ and could in principle deteriorate the precision of $cdc25^{string}$ transcriptional control. We speculate that $Cdc25^{string}$-driven switches similar to the one that we have described might be a preferred solution for the precise temporal control of mitosis (O'Farrell, 2001). Such switches, when operating as short-term integrators, have the ability to filter out the probably unavoidable fast fluctuations in the expression of $cdc25^{string}$.

Transcriptionally Driven Covalent Modification Cycle as a Mechanism to Precisely Control Cell Decisions

Covalent modification cycles are widespread signaling modules that can generate ultrasensitivity when operating in the zero-order regime (Goldbeter and Koshland, 1981; Kholodenko, 2006). Our theoretical work shows that transcriptionally driven covalent modification cycle can effectively generate an ultrasensitive response when they operate in the first-order regime as long as they are not close to steady state. In this regime, these cycles also display interesting signaling properties (Detwiler et al., 2000; Gomez-Uribe et al., 2007). They act as low-pass filters dampening fluctuations that happen on time scales faster than the response time (Detwiler et al., 2000; Gomez-Uribe et al., 2007). Effectively, they resemble short-term integrators with an integration time that is determined by the response time. Because the response time depends on the concentration of the two opposing enzymes, the filtering properties of the cycle can be easily tuned to the desired frequency (Detwiler et al., 2000; Gomez-Uribe et al., 2007). We propose that by driving the cycle with $cdc25^{string}$ expression, *Drosophila* is able to achieve switch-like behavior while maintaining the robust filtering properties of covalent modification cycles. Positive feedback driven circuits that have similar integration properties and therefore achieve both ultrasensitive and precise control of cell decision might be much harder to design. We speculate that covalent modification cycles, triggered by transcriptional expression of the activating enzymes, might be a widespread strategy to obtain reliable and switch-like control of cell decisions.

EXPERIMENTAL PROCEDURES

Fly Stocks and Plasmids

Standard methods were used all throughout. To distinguish $cdc25^{string}$ heterozygous embryos from WT embryos, we crossed His2Av-RFP females to males carrying the $cdc25^{string}$ amorphic allele stg^{7M53} on one chromosome and a $cdc25^{string}$ enhancer driving GFP-NLS on the other. This cross produces WT embryos (GFP positive) and embryos heterozygous for $cdc25^{string}$ (GFP negative).

Microscopy

Live imaging of His2Av-GFP embryos was performed on a CARV spinning disk confocal microscope (Nikon) using a X-Cite120Q light source and a CCD camera (Hamamatsu ORCA-ER). Images were acquired every 20 s. The other live imaging experiments were performed with a Leica SP5 confocal microscope, a 20×/0.7 numerical aperture glycerol-immersion objective, an argon ion laser and a 594-nm diode laser. Detection was performed using photomultiplier tubes. For embryos expressing GFP and RFP every acquired image was the average of 30 subsequent images (acquired with a scanning time slightly larger than 1 s for an image 1,024 × 512 pixels, giving a frame rate of 40 s). For embryos expressing CFP, GFP, and RFP every acquired image was the average of 20 subsequent images (acquired with a scanning time of about 2 s for an image 1,024 × 512 pixels, giving a frame rate of 40 s). Averaging was used to obtain a good signal-to-noise ratio and minimize photobleaching.

Image Analysis

Using MATLAB (MathWorks) we developed software to track nuclei and measure fluorescence intensity. Mitotic events were scored manually.

Data Analysis

The time of transcriptional activation of *cdc25^{string}enh-GFP* (Figure 2) was evaluated using the method described in Skotheim et al. (2008).

We used the UAS/Gal4 system to uniformly express fluorescently tagged Cdc25^{string} or Cdc25^{string}9A (in some experiments coexpressed with Wee1 and Wee19A respectively) and obtain quantitative dynamical data on how the rate of entering mitosis depends on Cdc25^{string} dynamics. We imaged various embryos of the appropriate genotypes and obtained all our quantitative data from single embryos in order to avoid possible global differences between the embryos (e.g., different transcription\translation rates in different embryos). We developed an algorithm to segment and track individual nuclei. The number of cells analyzed for each genotype was: *UAS-Cdc25^{string}GFP* 198 cells, *UAS-Cdc25^{string}9AGFP* 233 cells, *UAS-Cdc25^{string}GFP UAS-Wee1CFP* 148 cells, *UAS-Cdc25^{string}9AGFP UAS-Wee19ACFP* 110 cells, *UAS-Cdc25^{string}GFP* in *wee1* heterozygous (see Figure 7) 173 cells.

The measured fluorescence intensity of Cdc25^{string}GFP is not strictly proportional to its concentration because GFP does not mature instantaneously or on time scales significantly shorter than the time scale over which Cdc25^{string} accumulation controls entry into mitosis. Therefore, to estimate the concentration of Cdc25^{string}GFP from the measured fluorescence traces (i.e., correct for the maturation time of GFP), we used the following mathematical model:

$$\begin{aligned} \frac{ds}{dt} &= \beta(t) \quad -\frac{1}{\tau}s - \frac{1}{\tau_1}s \\ \frac{ds^*}{dt} &= \quad \frac{1}{\tau}s - \frac{1}{\tau_1}s^* \end{aligned}$$

where s indicates immature Cdc25^{string}GFP, s* indicates fluorescent Cdc25^{string}GFP, τ describes the pseudo-first-order kinetics of GFP maturation (Heim et al., 1995; Sniegowski et al., 2005), τ_1 describes the degradation dynamics of Cdc25^{string}GFP, assumed also to be first-order and $\beta(t)$ indicates the translation rate of Cdc25^{string}.

The total amount of Cdc25^{string}GFP, indicated as s_T, can be estimated from the measured fluorescence signal s* by the following expression: $s_T = s + s^* = s^*(1 + (\tau/\tau_1)) + \tau(ds^*/dt)$.

Algebraic conversion yields: $s_T \sim s^* + \gamma(ds^*/dt)$, where $\gamma = \tau\tau_1/(\tau + \tau_1)$. This equation implies that it is possible to infer Cdc25^{string} dynamics from the data without a detailed knowledge of the translation rate $\beta(t)$ (note that: min $(\tau,\tau_1)/2 \leq \gamma \leq$ min (τ,τ_1) and that $\gamma = 0$ min would correspond to not applying any correction to the measured intensities).

The measurement of Cdc25^{string}GFP fluorescence intensity displayed appreciable variability (Figure S2A). We used the smoothing spline in MATLAB (De Boor, 2001) with a parameter p = 0.1 to obtain Cdc25^{string}GFP intensity at any given time point rather than using the value directly measured. Figures S4A and S4B show that control of the cell cycle by Cdc25^{string} is switch-like regardless of the value of γ and thus very robust to changes in the parameters used to reconstruct Cdc25^{string}GFP concentration. Similarly, it can be shown that our conclusion that positive feedback does not play an important role in the control of mitosis is also very robust to the parameters used to reconstruct Cdc25^{string} dynamics (Figure S5).

To determine the integration time for the decision to enter mitosis, we reconstructed the dynamics of Cdc25^{string} using various values of γ and then studied how the integration time depends on this parameter. We found that there is a small range of parameters ($\gamma < 3.5$ min, see Figures S3A and S3B) compatible with an instantaneous model. For larger values of γ, the integration time sharply increases to a plateau of about 3.5 min (Figures S3A and S3B). Effectively values of γ between 8 and 360 min predict integration times that differ by less than a factor two (1.8–3.5 min). These results suggest that, as long as γ is larger than 8 min, the integration time for the decision of entering mitosis should be ~2–3 min and that such estimate is very robust to changes in the parameters used to reconstruct Cdc25^{string} dynamics.

To estimate γ experimentally, we measured the maturation time of GFP and the lifetime of Cdc25^{string}GFP (see Supplemental Experimental Procedures). We obtained a maturation time for GFP of 41 ± 6 min and a lifetime for Cdc25^{string} of 31 ± 4 min. From these estimates, we obtain $\gamma = 18 \pm 5$ min (integration time = 2.6 ± 1.0, Figures S3A and S3B) and thus conclude that 2–3 min is a reasonable estimate of the integration time relevant for the decision of entering mitosis.

Binning was performed by separating data in nonoverlapping bins and plotting the mean and the standard error for each bin. The rate of cell division as function of × was defined as the probability that a cell that has not yet divided would divide at a given value of × (× indicates Cdc25^{string}GFP or Cdc25^{string}-9AGFP). Operatively, we start from a histogram of × at entry into mitosis and then compute the ratio between the number of cells that divide within a given concentration interval and the total number of cells that had not divided yet. The error bars on the rate of cell division are standard errors, estimated assuming that the number of cells that divide within a given concentration interval follows a Bernoulli distribution.

For the analysis presented in Figure 3F, we separated cells in three subgroups according to their position along the anterior-posterior axis (anterior: cells occupying the region between 5% and 20%, middle: cells occupying the region between 43% and 58%, posterior: cells occupying the region between 80% and 95%).

Error bars for Hill coefficients and integration time represent 95% confidence intervals.

Western Blots

Standard methods (Maniatis et al., 1982) were used with the following primary antibodies: mouse anti-GFP antibody (1:1,000, Roche), rabbit anti-Cdk1pY15 antibody (1:1,000, Cell Signaling), Cdk1 p34(PSTAIRE) (1:200, Santa Cruz), mouse anti-αtubulin antibody (1:5,000, Sigma-Aldrich), and rat anti-Wee1 (1:1,000). A FluorChem HD2 system

(AlphaInnotech) was used to image and quantify the signals from the chemiluminescence reactions.

Recombinant Proteins and Estimate of Cdc25 Enzymatic Properties

GST-Cdk1 was expressed in *Escherichia coli* and purified using the method described in Frangioni and Neel (1993). Wee1 protein was purified by GenScript, purified recombinant GFP was purchased from Clontech.

To estimate the enzymatic properties of $Cdc25^{string}$, we observe that the k_{cat} of human Cdc25s and of their catalytic domains has been measured for various substrates and is close to 1 s^{-1} (Gottlin et al., 1996; McCain et al., 2002; Wilborn et al., 2001). Because on-rate for efficient enzymes range between 10^5–10^6 $M^{-1}s^{-1}$ (Chen et al., 2010), one can deduce that $K_m = (k_{cat} + k_{off})/k_{on} > 1\ \mu M$.

Antibody Production

Rat anti-Wee1 antisera were raised against purified full-length Wee1 protein by Panigen. Specificity of the antibodies was tested by comparing western blots of WT and *wee1-null* embryos.

Simulations

Differential equations describing the mitotic switch (Supplemental Experimental Procedures) were solved in MATLAB.

Supplementary Material

Refer to Web version on PubMed Central for supplementary material.

Acknowledgments

We thank the Drosophila Genomics Resource Center for plasmids and the Bloomington Drosophila Stock Center for fly stocks. We thank Shelagh Campbell, Fred Cross, Pat O'Farrell, James Ferrell, Margaret Fuller, Douglas Kellogg, David Morgan, Eric Siggia, Jan Skotheim, Massimo Vergassola, Ned Wingreen, and all the members of the Wieschaus and Schupbach laboratories for discussions. S.D. is a Howard Hughes Medical Institute Fellow of the Life Sciences Research Foundation. E.F.W. is an investigator of the Howard Hughes Medical Institute.

REFERENCES

Chen WW, Niepel M, Sorger PK. Classic and contemporary approaches to modeling biochemical reactions. Genes Dev. 2010; 24:1861–1875. [PubMed: 20810646]

Coudreuse D, Nurse P. Driving the cell cycle with a minimal CDK control network. Nature. 2010; 468:1074–1079. [PubMed: 21179163]

De Boor, C. A Practical Guide to Splines: With 32 Figures. Revised Edition. Springer; New York: 2001.

Deibler RW, Kirschner MW. Quantitative reconstitution of mitotic CDK1 activation in somatic cell extracts. Mol. Cell. 2010; 37:753–767. [PubMed: 20347419]

Detwiler PB, Ramanathan S, Sengupta A, Shraiman BI. Engineering aspects of enzymatic signal transduction: photoreceptors in the retina. Biophys. J. 2000; 79:2801–2817. [PubMed: 11106590]

Edgar BA, O'Farrell PH. Genetic control of cell division patterns in the Drosophila embryo. Cell. 1989; 57:177–187. [PubMed: 2702688]

Edgar BA, O'Farrell PH. The three postblastoderm cell cycles of Drosophila embryogenesis are regulated in G2 by string. Cell. 1990; 62:469–480. [PubMed: 2199063]

Edgar BA, Lehman DA, O'Farrell PH. Transcriptional regulation of string (cdc25): a link between developmental programming and the cell cycle. Development. 1994a; 120:3131–3143. [PubMed: 7720557]

Edgar BA, Sprenger F, Duronio RJ, Leopold P, O'Farrell PH. Distinct molecular mechanism regulate cell cycle timing at successive stages of Drosophila embryogenesis. Genes Dev. 1994b; 8:440–452. [PubMed: 7510257]

Fell DA. Metabolic control analysis: a survey of its theoretical and experimental development. Biochem. J. 1992; 286:313–330. [PubMed: 1530563]

Foe VE. Mitotic domains reveal early commitment of cells in Drosophila embryos. Development. 1989; 107:1–22. [PubMed: 2516798]

Frangioni JV, Neel BG. Solubilization and purification of enzymatically active glutathione S-transferase (pGEX) fusion proteins. Anal. Biochem. 1993; 210:179–187. [PubMed: 8489015]

Gavet O, Pines J. Progressive activation of CyclinB1-Cdk1 coordinates entry to mitosis. Dev. Cell. 2010; 18:533–543. [PubMed: 20412769]

Goldbeter A, Koshland DE Jr. An amplified sensitivity arising from covalent modification in biological systems. Proc. Natl. Acad. Sci. USA. 1981; 78:6840–6844. [PubMed: 6947258]

Gomez-Uribe C, Verghese GC, Mirny LA. Operating regimes of signaling cycles: statics, dynamics, and noise filtering. PLoS Comput. Biol. 2007; 3:e246. [PubMed: 18159939]

Gottlin EB, Xu X, Epstein DM, Burke SP, Eckstein JW, Ballou DP, Dixon JE. Kinetic analysis of the catalytic domain of human cdc25B. J. Biol. Chem. 1996; 271:27445–27449. [PubMed: 8910325]

Harvey SL, Charlet A, Haas W, Gygi SP, Kellogg DR. Cdk1-dependent regulation of the mitotic inhibitor Wee1. Cell. 2005; 122:407–420. [PubMed: 16096060]

Harvey SL, Enciso G, Dephoure NE, Gygi SP, Gunawardena J, Kellogg DR. A phosphatase threshold sets the level of Cdk1 activity in early mitosis in budding yeast. Mol. Biol. Cell. 2011; 22:3595–3608. [PubMed: 21849476]

Heim R, Cubitt AB, Tsien RY. Improved green fluorescence. Nature. 1995; 373:663–664. [PubMed: 7854443]

Hoffmann I, Clarke PR, Marcote MJ, Karsenti E, Draetta G. Phosphorylation and activation of human cdc25-C by cdc2—cyclin B and its involvement in the self-amplification of MPF at mitosis. EMBO J. 1993; 12:53–63. [PubMed: 8428594]

Izumi T, Maller JL. Elimination of cdc2 phosphorylation sites in the cdc25 phosphatase blocks initiation of M-phase. Mol. Biol. Cell. 1993; 4:1337–1350. [PubMed: 7513216]

Johnston LA. The trouble with tribbles. Curr. Biol. 2000; 10:R502–R504. [PubMed: 10898974]

Kholodenko BN. Cell-signalling dynamics in time and space. Nat. Rev. Mol. Cell Biol. 2006; 7:165–176. [PubMed: 16482094]

Kim SY, Ferrell JE Jr. Substrate competition as a source of ultrasensitivity in the inactivation of Wee1. Cell. 2007; 128:1133–1145. [PubMed: 17382882]

Kim SY, Song EJ, Lee KJ, Ferrell JE Jr. Multisite M-phase phosphorylation of Xenopus Wee1A. Mol. Cell. Biol. 2005; 25:10580–10590. [PubMed: 16287869]

Koshland DE Jr. Némethy G, Filmer D. Comparison of experimental binding data and theoretical models in proteins containing subunits. Biochemistry. 1966; 5:365–385. [PubMed: 5938952]

Kumagai A, Dunphy WG. Regulation of the cdc25 protein during the cell cycle in Xenopus extracts. Cell. 1992; 70:139–151. [PubMed: 1623517]

Lehman DA, Patterson B, Johnston LA, Balzer T, Britton JS, Saint R, Edgar BA. Cis-regulatory elements of the mitotic regulator, string/Cdc25. Development. 1999; 126:1793–1803. [PubMed: 10101114]

Maniatis, T.; Fritsch, EF.; Sambrook, J. Molecular Cloning: A Laboratory Manual. Cold Spring Harbor Laboratory; Cold Spring Harbor, NY: 1982.

McCain DF, Catrina IE, Hengge AC, Zhang ZY. The catalytic mechanism of Cdc25A phosphatase. J. Biol. Chem. 2002; 277:11190–11200. [PubMed: 11805096]

McGowan CH, Russell P. Cell cycle regulation of human WEE1. EMBO J. 1995; 14:2166–2175. [PubMed: 7774574]

Morgan, DO. The Cell Cycle: Principles of Control. New Science Press; London: 2007.

Mueller PR, Coleman TR, Dunphy WG. Cell cycle regulation of a Xenopus Wee1-like kinase. Mol. Biol. Cell. 1995; 6:119–134. [PubMed: 7749193]

Novak B, Tyson JJ. Numerical analysis of a comprehensive model of M-phase control in Xenopus oocyte extracts and intact embryos. J. Cell Sci. 1993; 106:1153–1168. [PubMed: 8126097]

O'Farrell PH. Triggering the all-or-nothing switch into mitosis. Trends Cell Biol. 2001; 11:512–519. [PubMed: 11719058]

Okamoto K, Sagata N. Mechanism for inactivation of the mitotic inhibitory kinase Wee1 at M phase. Proc. Natl. Acad. Sci. USA. 2007; 104:3753–3758. [PubMed: 17360425]

Parker LL, Atherton-Fessler S, Lee MS, Ogg S, Falk JL, Swenson KI, Piwnica-Worms H. Cyclin promotes the tyrosine phosphorylation of p34cdc2 in a wee1+ dependent manner. EMBO J. 1991; 10:1255–1263. [PubMed: 1850698]

Pomerening JR, Sontag ED, Ferrell JE Jr. Building a cell cycle oscillator: hysteresis and bistability in the activation of Cdc2. Nat. Cell Biol. 2003; 5:346–351. [PubMed: 12629549]

Pomerening JR, Kim SY, Ferrell JE Jr. Systems-level dissection of the cell-cycle oscillator: bypassing positive feedback produces damped oscillations. Cell. 2005; 122:565–578. [PubMed: 16122424]

Sha W, Moore J, Chen K, Lassaletta AD, Yi CS, Tyson JJ, Sible JC. Hysteresis drives cell-cycle transitions in Xenopus laevis egg extracts. Proc. Natl. Acad. Sci. USA. 2003; 100:975–980. [PubMed: 12509509]

Skotheim JM, Di Talia S, Siggia ED, Cross FR. Positive feedback of G1 cyclins ensures coherent cell cycle entry. Nature. 2008; 454:291–296. [PubMed: 18633409]

Sniegowski JA, Lappe JW, Patel HN, Huffman HA, Wachter RM. Base catalysis of chromophore formation in Arg96 and Glu222 variants of green fluorescent protein. J. Biol. Chem. 2005; 280:26248–26255. [PubMed: 15888441]

Solomon MJ, Glotzer M, Lee TH, Philippe M, Kirschner MW. Cyclin activation of p34cdc2. Cell. 1990; 63:1013–1024. [PubMed: 2147872]

Strausfeld U, Fernandez A, Capony JP, Girard F, Lautredou N, Derancourt J, Labbe JC, Lamb NJ. Activation of p34cdc2 protein kinase by microinjection of human cdc25C into mammalian cells. Requirement for prior phosphorylation of cdc25C by p34cdc2 on sites phosphorylated at mitosis. J. Biol. Chem. 1994; 269:5989–6000. [PubMed: 8119945]

Sveiczer A, Novak B, Mitchison JM. The size control of fission yeast revisited. J. Cell Sci. 1996; 109:2947–2957. [PubMed: 9013342]

Trunnell NB, Poon AC, Kim SY, Ferrell JE Jr. Ultrasensitivity in the Regulation of Cdc25C by Cdk1. Mol. Cell. 2011; 41:263–274. [PubMed: 21292159]

Wilborn M, Free S, Ban A, Rudolph J. The C-terminal tail of the dual-specificity Cdc25B phosphatase mediates modular substrate recognition. Biochemistry. 2001; 40:14200–14206. [PubMed: 11714273]

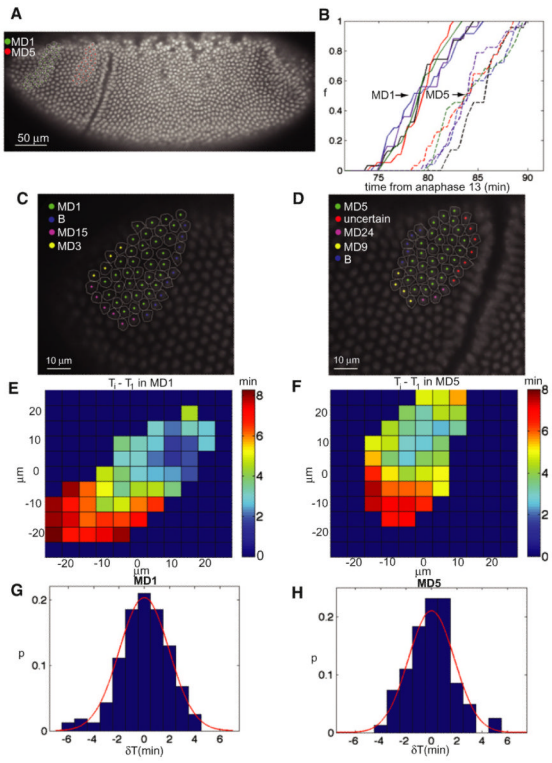

Figure 1. Mitosis inside Domains 1 and 5 Follow Reproducible Wave-Like Pattern

(A) Confocal image of His2Av-GFP embryo. Cells belonging to mitotic domain 1 (MD1) and mitotic domain 5 (MD5) are highlighted in green and red, respectively.

(B) Fraction of cells that have divided inside MD1 and MD5 as a function of time from anaphase 13.

(C and D) Enlarged view of a region around MD1 (C) and MD5 (D).

(E and F) A map of the average pattern of mitosis inside MD1 (E) and MD5 (F). Data show the time of cell division relative to the first cell that divides in the domain. The coordinates are relative to the centroid of the domain. Embryos were oriented laterally.

(G and H) Probability distribution of the difference (δT) between the time when a cell divides and the time when it was predicted to divide based on the average pattern; MD1 (G), MD5 (H). The data in both histograms are well described by a Gaussian (red lines) of standard deviation of ~2 min.

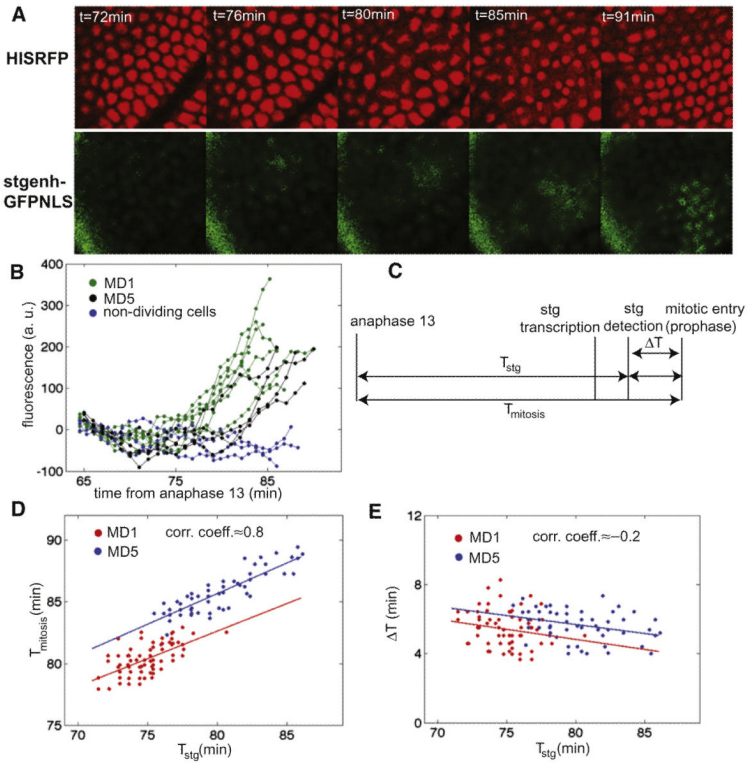

Figure 2. Transcriptional Activation of *cdc25*^{string} Controls the Wave-Like Pattern of Cell Divisions inside Mitotic Domain 1 and 5

(A) Confocal images of an embryo expressing His2Av-RFP and the transcriptional reporter for *cdc25*^{string} expression (*stgenh-GFPNLS*). The region displayed is the one surrounding MD5.

(B) Quantification of fluorescence intensity from *stgenh-GFPNLS* in individual cells.

(C) Diagram of the measured time intervals.

(D) Correlation between T_{stg} and $T_{mitosis}$ for cells in mitotic domain 1 (MD1, red circles) and in mitotic domain 5 (MD5, blue circles).

(E) Correlation between T_{stg} and ΔT for cells in mitotic domain 1 (MD1, red circles) and in mitotic domain 5 (MD5, blue circles). See also Figure S1 and Movie S1.

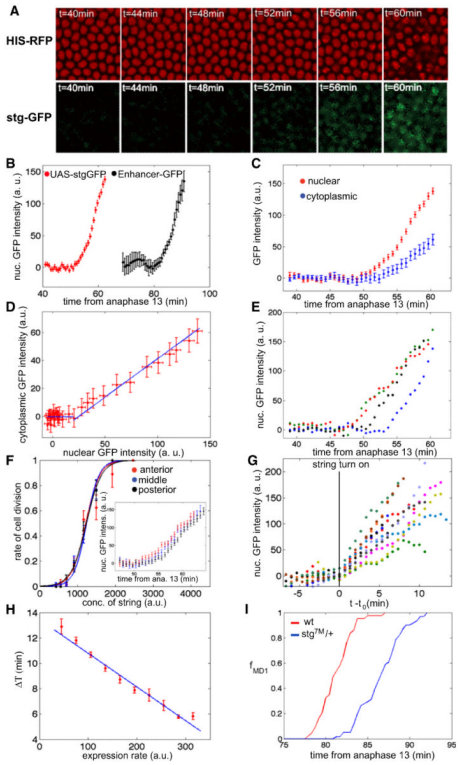

Figure 3. Cdc25^{string} Dynamics Controls Entry into Mitosis

(A) Confocal images of His2Av-RFP and UAS-Cdc25^{string}GFP (stgGFP) embryo.

(B) Average expression of UAS-Cdc25^{string}GFP and of stgenh-GFPNLS reporter as a function of time from anaphase 13 (the two data sets are from two separate embryos).

(C) Nuclear and cytoplasmic concentration of Cdc25^{string}GFP as a function of time from anaphase 13 (average of all the cells).

(D) Correlation between nuclear and cytoplasmic concentration derived from (C).

(E) Quantification of fluorescence intensity for individual cells.

(F) Rate of cell division as a function of Cdc25^{string}GFP concentration for cells in different positions along the anterior-posterior axis. Inset shows the average expression of UAS-Cdc25^{string}GFP for cells in different positions along the anterior-posterior axis.

(G) Quantification of fluorescence intensity of UAS-Cdc25^{string}GFP for individual cells with time rescaled to the beginning of Cdc25^{string}GFP accumulation (stg turn on, t_0).

(H) Correlation between ΔT (see Figure 2 for a definition) and the average expression rate of UAS-Cdc25^{string}GFP.

(I) Fraction of cells that have divided inside mitotic domain 1 as a function of time from anaphase 13 for WT embryos (red line) and embryos heterozygous for *cdc25^{string}* (blue line). Each curve is the average of data from five different embryos. Error bars are standard error of the mean. See also Figure S2 and Movie S2.

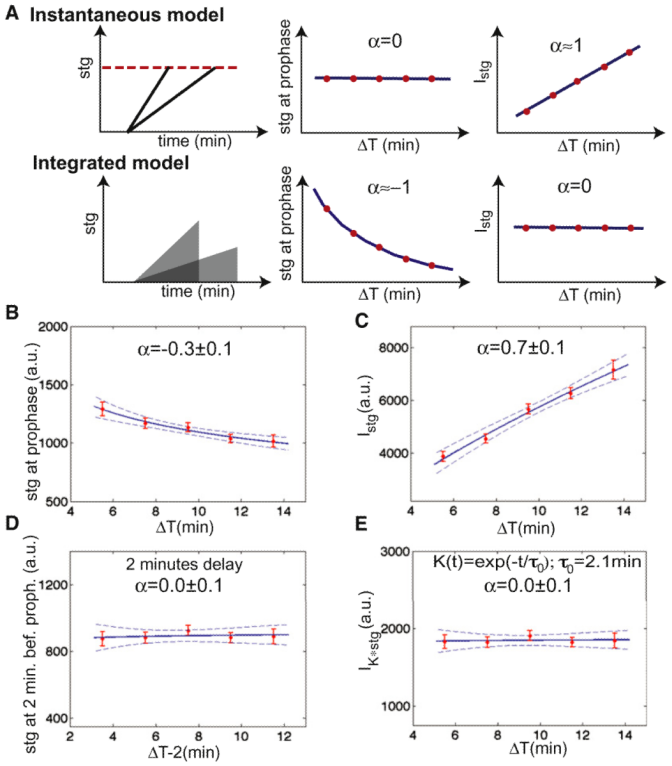

Figure 4. Two Models for the Control of Entry into Mitosis

(A) Correlation analysis to distinguish between an instantaneous and an integrated model for cell cycle control. Data were fitted with the function $A\Delta T^{\alpha}$ (predicted value of α are reported; dashed lines are 95% confidence intervals on the fit).

(B) Concentration of $Cdc25^{string}$ at the time of chromosome condensation as a function of ΔT.

(C) Integral of the concentration of $Cdc25^{string}$ as a function of ΔT.

(D) Concentration of $Cdc25^{string}$ 2 min before chromosome condensation as a function of ΔT.

(E) Convolution between the concentration of $Cdc25^{string}$ and an exponential kernel K(t) as a function of ΔT $\left(I_{k^*stg}=\int_0^{\Delta T} stg\left(t'\right)e^{-\left(\Delta T-t'\right)/\tau_0}dt'\right)$, where t = 0 is the beginning of $Cdc25^{string}$ accumulation. Error bars are standard error of the mean. See also Figure S3.

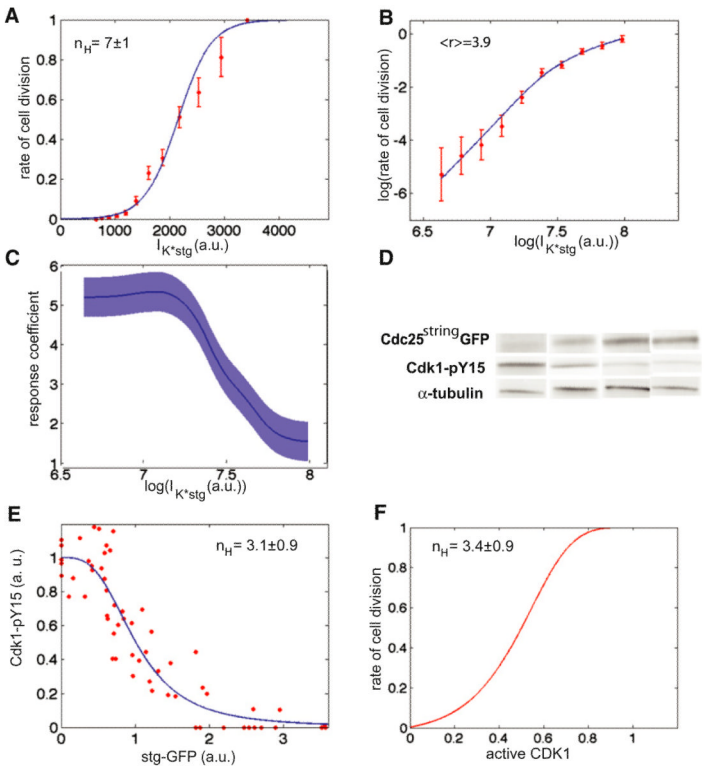

Figure 5. Cdc25^{string} Controls Entry into Mitosis and Cdk1 Activation in a Switch-like Manner

(A) Rate of cell division as a function of I_{K*stg}. The fit gives an apparent Hill coefficient $n_H = 7 \pm 1$.

(B) Log-log plot of the rate of cell division as a function of I_{K*stg}.

(C) Response coefficient r as a function of I_{K*stg}.

(D) Detection of Cdc25^{string}GFP and Cdk1-pY15 by western blot of individual embryos.

(E) Quantification of Cdk1-pY15 amount as a function of Cdc25^{string}GFP (stgGFP) amount. The line is a Hill function with coefficient $n_H = 3.1 \pm 0.9$.

(F) Rate of cell division as a function of Cdk1 activity. This dependency was derived using the dependency of the rate of cell division (A) and of Cdk1 activity (D) on Cdc25^{string} concentration (a relation between the two different measurements of Cdc25^{string} was inferred by measuring Cdc25^{string}GFP and Cdk1-pY15 levels in embryos in which approximately half of the cells were in mitosis). Error bars are standard error of the mean. See also Figure S4.

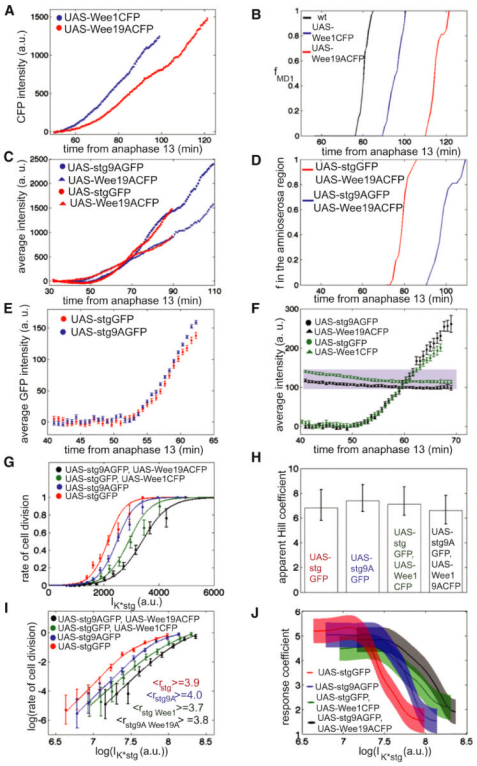

Figure 6. Switch-like Control of Mitotic Entry Is Independent of Feedbacks

(A) Fluorescence intensity of zygotically expressed UAS-Wee1CFP (blue points) and UAS-Wee19ACFP (red points) as a function of the time from anaphase 13.

(B) Fraction of UAS-Wee1CFP (blue line), UAS-Wee19ACFP (red line), and WT (black line) cells that have divided inside mitotic domain 1 as a function of time from anaphase 13.

(C) Fluorescence intensity of zygotically expressed UAS-Wee19ACFP UAS-Cdc25^{string}GFP (red triangles and circles, respectively) and UAS-Wee19ACFP UAS-Cdc25^{string}9AGFP (blue triangles and circles, respectively) as a function of the time from anaphase 13.

(D) Fraction of UAS-Wee19ACFP UAS-Cdc25^{string}GFP (red line) and UAS-Wee19ACFP UAS-Cdc25^{string}9AGFP (blue line) cells that have divided in the amnioserosa region as a function of the time from anaphase 13.

(E) Average expression of UAS-Cdc25^{string}GFP (red circles) and of UAS-Cdc25^{string}9AGFP (blue circles) as a function of time from anaphase 13.

(F) Average expression of UAS-Cdc25^{string}GFP (green circles), UAS-Wee1CFP (green squares), UAS-Cdc25^{string}9AGFP (black circles), and UAS-Wee19ACFP (black squares) as a function of time from anaphase 13. Shaded region indicates the expression levels of endogenous Wee1.

(G) Rate of cell division as a function of I_{K*stg} (UAS-Cdc25^{string}GFP, red circles; UAS-Cdc25^{string}GFP UAS-Wee1CFP green circles; UAS-Cdc25^{string}9AGFP, blue circles; UAS-Cdc25^{string}9AGFP, UAS-Wee19ACFP, black circles).

(H) Bar graph reporting the apparent Hill coefficients for all four data sets reported in (G).

(I) Log-log plot of the rate of cell division as a function of I_{K*stg} (UAS-Cdc25^{string}GFP, red circles; UAS-Cdc25^{string}GFP, UAS-Wee1CFP, green circles; UAS-Cdc25^{string}9AGFP, blue circles; UAS-Cdc25^{string}9AGFP, UAS-Wee19ACFP, black circles). The numbers reported in the graph are the average response coefficients.

(J) Response coefficient r as a function of I_{K*stg} for all four data sets reported in (I). Error bars are standard error of the mean, with exception of (H) where the 95% confidence interval is reported. See also Figure S5 and Movies S3, S4, S5, and S6.

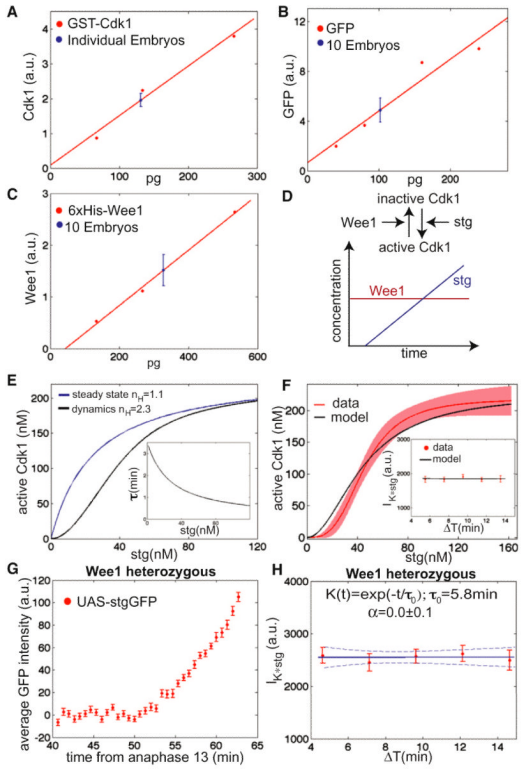

Figure 7. A Covalent Modification Cycle Operating Out-of-Equilibrium and as a Short-Term Integrator Controls Entry into Mitosis

(A) Quantification of western blot of individual embryos and recombinant GST-Cdk1.

(B) Quantification of western blot of ten UAS-Cdc25^{string}GFP embryos and recombinant GFP. Fraction of inactive Cdk1 (Cdk1-pY15) was measured comparing the ratio of Cdk1-pY15 over tubulin to the same ratio measured in embryos in G2 of cycle 14 (mid cellularization).

(C) Quantification of western blot of ten embryos in G2 of cycle 14 and recombinant 6xHis-Wee1.

(D) Schematic representation of the mathematical model.

(E) Simulations of Cdk1 activation by a covalent modification cycle controlled by Cdc25^{string} and Wee1. Inset shows the response time (τ) as a function of Cdc25^{string} concentration.

(F) Measured (Figure 5D) and simulated Cdk1 activation as a function of Cdc25^{string} concentration (shaded region indicates the 95% confidence interval of the fit of the experimental data). Inset shows I_{K^*stg} (as defined in Figure 4) as a function of ΔT for experimental data and numerical simulations.

(G) Average nuclear intensity of UAS-Cdc25^{string}GFP as a function of time from anaphase 13 for an embryo heterozygous for *wee1*.

(H) I_{K^*stg} (computed using an integration time τ_0 = 5.8 min) as a function of ΔT for the *wee1* heterozygous embryo. Dashed lines are 95% confidence intervals on the fit. Error bars are standard error of the mean.

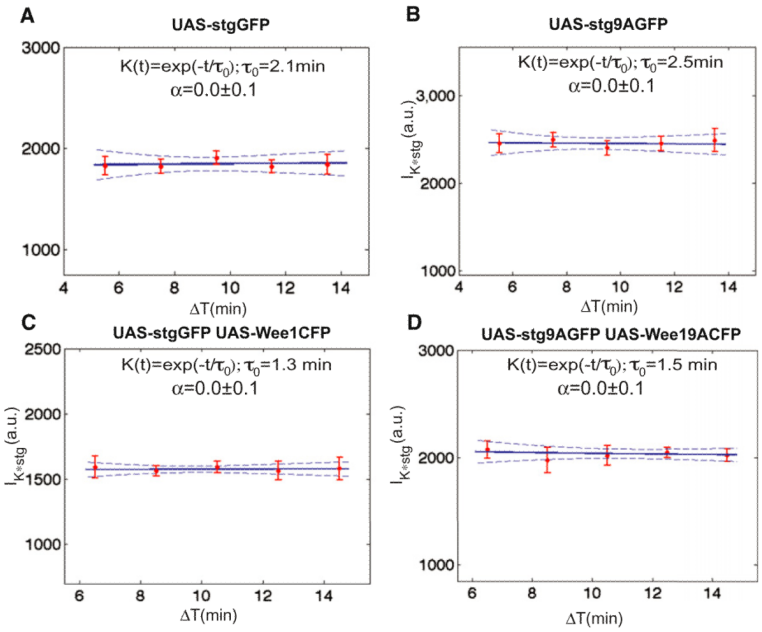

Figure 8. The Integration Time Does Not Depend on Positive Feedback

Convolution between the concentration of Cdc25^{string} and an exponential kernel K(t) as a function of ΔT $\left(I_{k^*stg}=\int_0^{\Delta T} stg\left(t'\right)e^{-\left(\Delta T-t'\right)/\tau_0}dt'\right)$ for UAS-Cdc25^{string}GFP (A), UAS-Cdc25^{string}9AGFP (B), UAS-Cdc25^{string}GFP UAS-Wee1CFP (C), and UAS-Cdc25^{string}9AGFP UAS-Wee19ACFP (D). The data are from the same embryos shown in Figure 6. Expression of either Cdc25^{string} or Cdc25^{string}9A produces comparable integration times. Compare (A) and (B) integration times: 2.1 ± 0.9 min and 2.5 ± 0.9 min, respectively. The integration time decreases with ectopic Wee1 expression (compare C and D with A and B), but is very similar in embryos expressing either the WT and mutant Wee1 protein (integration times: 1.3 ± 0.7 min and 1.5 ± 0.8 min respectively), indicating that the relative contribution of positive feedback is minor compared to the contribution of the balance between the two components. Error bars are standard error of the mean, dashed lines are 95% confidence interval on the fit.